PULSAR RECEPTION AT 22 MHZ

by

P. DEWDNEY

B.A.Sc. in Engineering Physics, University of B.C., 1968

A THESIS SUBMITTED IN PARTIAL FULFILMENT OF

THE REQUIREMENTS FOR THE DEGREE OF

MASTER OF APPLIED SCIENCE

in the Department of

Electrical Engineering

We accept this thesis as conforming to the

required standard

Research Supervisor..

Members of the Committee....................................

....

Acting Head of the Department...............................

Members of the Department

of Electrical Engineering

THE UNIVERSITY OF BRITISH COLUMBIA

January, 1970

In presenting this thesis in partial fulfilment of the requirements for an advanced degree at the University of British Columbia, I agree that the Library shall make it freely available for reference and study. I further agree tha permission for extensive copying of this thesis for scholarly purposes may be granted by the Head of my Department or by his representatives. It is understood that copying or publication of this thesis for financial gain shall not be allowed without my written permission.

Department of Electrical Engineering

The University of British Columbia
Vancouver 8, Canada

Date Jan 16, 1970

ABSTRACT

An attempt is made to receive pulsar signals at a frequency (22 MHz) lower than they have been received before. The problem of high galactic background radiation is the dominant one. The receiver used optimizes the ratio of signal to sky background noise.

The technique uses the property that pulsar signals are dispersed by intervening electrons. Using the known dispersion relation it is possible to predict the phase of the pulsar signal at one frequency (22 MHz) if it is known at another frequency (150 MHz). The receiver then tracks the pulse in frequency vs. time with a bandwidth which is small enough to match the instantaneous bandwidth of the signal.

Although it was found that pulsar signals from CP 1919 are still too weak to be received on such a system, an upper limit to their strength was obtained by measuring its sensitivity. At the time of observation (August, 1969) the signal strength at 22 MHz, averaged over 2600 pulses, was less than 1.0×10^{-26} joules per m^2 of capture cross-section per unit bandwidth.

TABLE OF CONTENTS

LIST OF ILLUSTRATIONS

ACKNOWLEDGEMENT

I wish to thank Professor F.K. Bowers for his guidance and encouragement in carrying out this research. Furthermore, I would like to thank the staff of the Dominion Radio Astrophysical Observatory for their assistance and encouragement, and to acknowledge the use of facilities there.

This research was conducted with the financial assistance from a National Research Council bursary and from National Research Council grant A-3295 given to the Department of Electrical Engineering at the University of British Columbia.

1. PULSARS

Since pulsars were discovered in 1968 by Hewish et al. at Cambridge, much work has been done to measure the properties of known pulsating sources, and to search for new ones.[1] Pulsar signals exhibit very unusual properties. At the source they are pulses of radio frequency noise which are emitted over a very broad range of frequencies (from 40 MHz to a few GHz). The pulse repetition rate is exceedingly constant (to within at least one part in 10^7 per year)[2]. Although it has been presumed that the pulses are emitted simultaneously on all frequencies, it has been found that pulsar signals observed on a low frequency are delayed with respect to those observed on a high frequency. Investigations of this phenomenon have shown that there is dispersion caused by intervening electrons along the line of sight to the pulsar. The measured dispersion accurately fits the relation

$$\frac{df}{dt} = -\frac{f^3 c}{\int f_p^2 dL}$$

where f is the received frequency

c is the velocity of light

f_p is the plasma frequency ($f_p = 8.98 \times 10^{-3} \, n_e^{\frac{1}{2}}$)

n_e is the electron density in the intervening medium

dL is an increment of distance along the line of sight,

or

$$\frac{df}{dt} = 1.2048 \times 10^{-4} \frac{f^3}{\int n_e \, dL}$$

where f is in MHz

n_e is in electrons-cm^{-3}.

$\int n_e \, dL$ is known as the dispersion measure and is usually quoted in parsec-cm^{-3} (1 parsec = 3.26 light- years). An illustration of the shape of the frequency vs. time curve of observed pulsar signal is shown in Figure 1-1. In this model the pulse width is independent of frequency. There has been some evidence that the duration of the observed pulse is longer at low frequencies than at high ones. The effect is small but requires a more complicated theoretical explanation of the dispersion [4]. Among the pulsars there is quite a wide range of pulse repetition rates and pulse durations. The fastest repetition rate is about 30 per second; the slowest is about 1 every 4 seconds. The pulse widths vary from 2 msec to 200 msec. The fastest repetition rates are usually accompanied by the longest pulse durations. Pulsar signals received at 408 MHz can be seen in Figure 1-2.

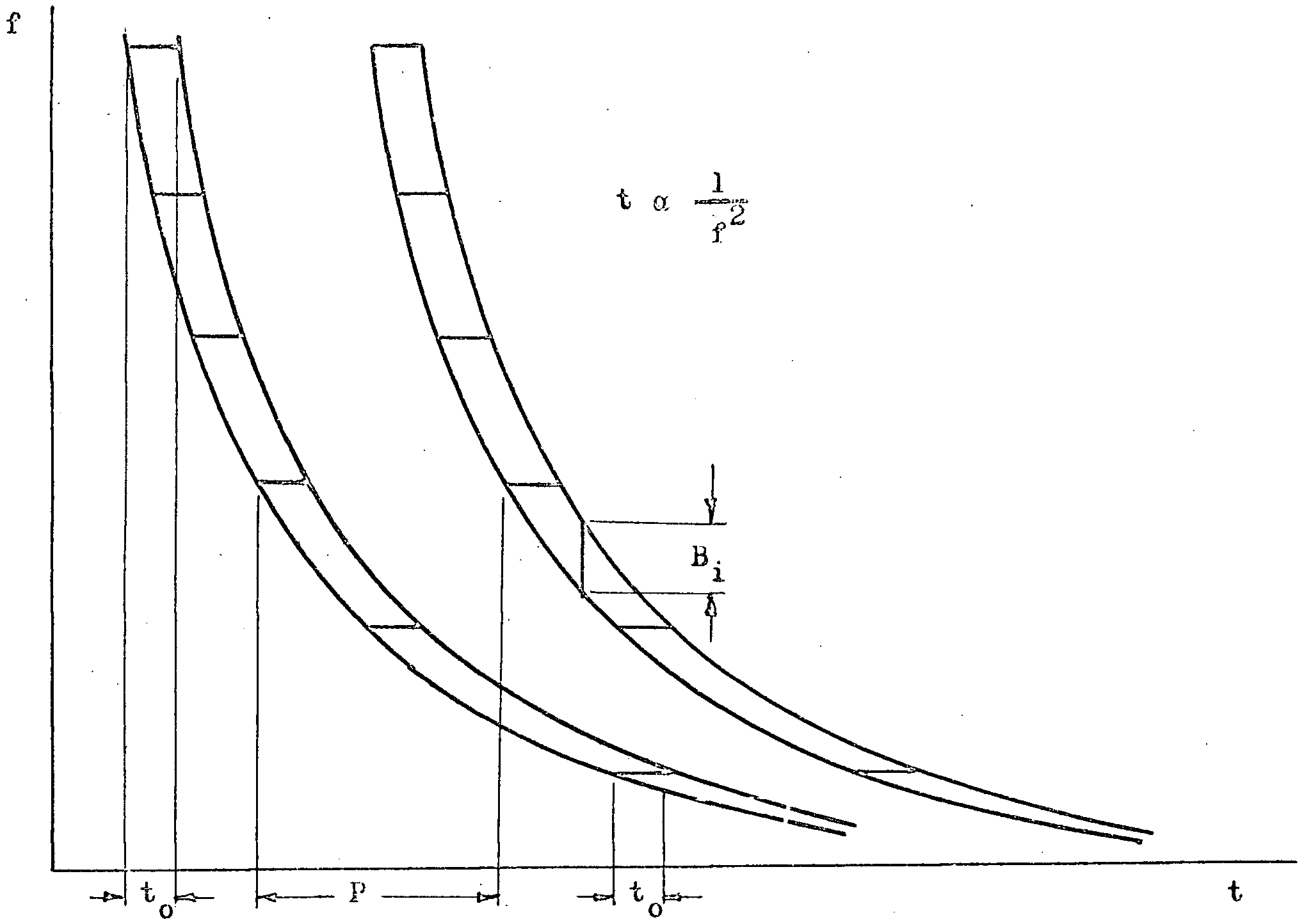

Figure 1-1
The pulsar signal sweep (not to scale). t_o is the pulse width (constant with frequency). P is the pulsar period. B_i is the instanteous bandwidth.

The radio frequency spectra of the pulsar signals are very difficult to obtain because of the large, random variations in the intensity of the pulses. Some histograms of intensity distributions have been measured for the pulsar CP 1919. (For the designation of pulsars see reference 4) A measured distribution can be seen in reference 5. The distribution function decays exponentially at intensities above the average intensity. This type of distribution has been observed at several frequencies by Lovelace and Craft at Arecibo Ionospheric Observatory. Pulses outside a small frequency range do not seem to be correlated in intensity. For instance, at 430 MHz correlation was observed only in a range of about 3 MHz for CP 1919.

Figure 1-2
Pulsar signals received at 408 MHz.

The method of expressing pulsar signal intensity varies slightly in the literature. The intensity will be taken here to mean the total energy per average pulse striking a unit capture cross-section per unit bandwidth. The intensities quoted in the literature have been standardized to this form. Where necessary pulse widths for this standardization have been taken from reference 4.

Some spectra are plotted in Figure 1-3 for CP 1919. The wide range of intensities is due partly to the different averaging techniques used by the various observers, and partly due to the large, long-term variations in pulsar signal strength. Each spectrum in Figure 1-3 is denoted by a letter and a number. The letter stands for the observatory where the spectrum was measured. The number is the number of pulse periods used to obtain the average. Spectra which have been drawn from selected large pulses or groups of such pulses are noted. Inevitably, there will be some selection effect because weak pulses will be lost in background noise. Note that although there are shifts of overall level, the shapes of the spectra measured by different observatories are similar. (with the exception of one point on the Parkes spectrum).

Periods quoted in the literature are usually referred to the earth-sun barycentre. Owing to the motion of an earthbound observer with respect to this point, the period will be doppler-shifted. The earth's orbital motion contributes most of this effect but there is also a daily variation due to its axial rotation.

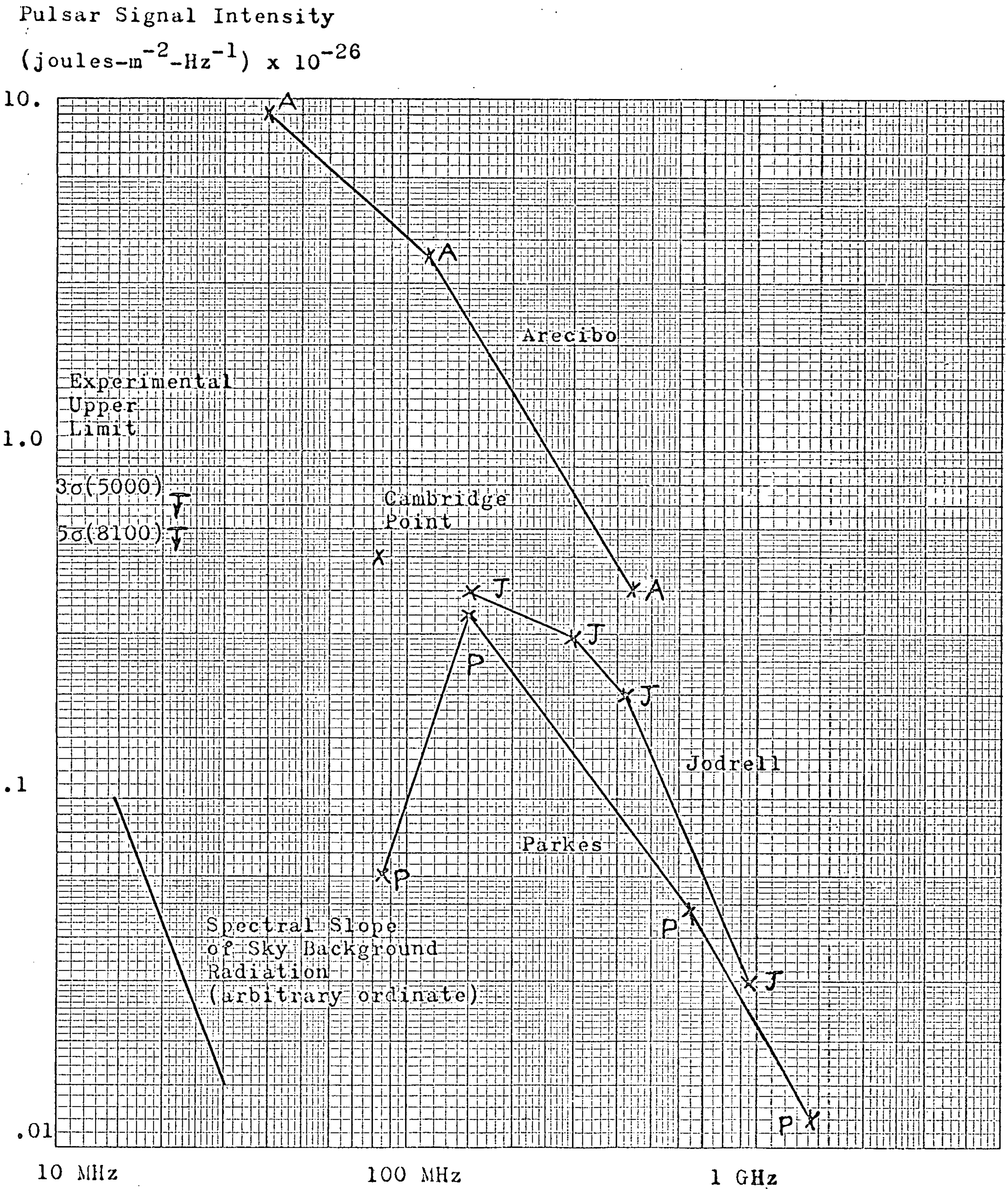

Pulsar Signal Intensity
(joules-m^{-2}-Hz^{-1}) x 10^{-26}
10.
1.0
.1
.01
10 MHz
100 MHz
1 GHz
Arecibo
Experimental
Upper
Limit
3σ(5000)
5σ(8100)
Cambridge
Point
Jodrell
Parkes
Spectral Slope
of Sky Background
Radiation
(arbitrary ordinate)
A
J
P

Figure 1-3

Note 1: The Parkes spectrum represents a 5000 pulse average. At 85 MHz identification of pulses less than .3 x 10^{-26} joules-m^{-2}-Hz^{-1} was reported to be very difficult. However, the average was determined to be .06 x 10^{-26} joules-m^{-2}-Hz^{-1}. Because many of the low energy pulses may have been excluded from this average, it may be lower than one which includes these pulses.

Note 2: The Arecibo spectrum is a 6144 pulse average at 111.5 MHz, and a 4096 pulse average at 430 MHz. At 111.5 MHz Arecibo reports that there is a variation in 6 equal subdivisions of the data of .85 to 1.3 times the average. Similarly, in 4 equal subdivisions at 430 MHz the range was from .4 to 1.6 times the average.[5] At 40 MHz three observations of 4096, 754, and 3940 pulses were averaged. The range was from .2 to 1.6 times this average.(private letter) Because these intensities were reported as peak flux, a factor of 1/ 2 was introducted to determine the mean pulse height.

Note 3: The Jodrell spectrum is an average over approximately 8100 pulses.[15] Included in this spectrum at 82 MHz is a Cambridge measurement.[1]

Note 4: At 22 MHz the level of three standard deviations of the noise level has been indicated for a 5000 and 8100 pulse average as an upper limit for comparison with the other spectra.

2. JUSTIFICATION OF THE EXPERIMENT

There are no observations of any of the pulsar spectra at frequencies less than 40 MHz, and the work done at frequencies less than 80 MHz is very limited.[3] Although the data are very incomplete, it appears that the pulsar intensity may be less than 10^{-25} joules-m^{-2}-Hz^{-1} at 22 MHz.(see Figure 1-3). The availability of a large antenna at this frequency at the Dominion Radio Astrophysical Observatory near Penticton, B.C. makes detection in this flux density range feasible. The physical area of this antenna is 23,693 m^2. It is comparable to the collecting area of Arecibo Ionospheric Observatory's circular dish at this frequency. Even an upper limit in this sensitivity range would be sufficiently low to be of use in determining the slope of the spectra of pulsar signals at low frequencies. A spectral cutoff at low frequencies would be useful in restricting theories of the origin of pulsar signals. Also, since the dispersion is proportional to the inverse square of the frequency, a measurement of the delay from frequencies above 100 MHz would give a very accurate dispersion measure. Thirdly, as indicated in chapter 1, there is some evidence that the pulse gets systematically wider as the frequency decreases. Previously, it had been thought that the pulse width was independent of frequency. Detection of the pulsar signals at 22 MHz would be a sensitive measure of this trend. These considerations provide the basis of justification of the experiment described herein.

3. SIGNAL-TO-NOISE PROBLEM

At frequencies near 22 MHz the background noise from the sky is considerable. The "coldest" part of the sky is about 40,000 degrees of brightness temperature. In the plane of the Galaxy the sky brightness temperature rises as high as 280,000 degrees.[13] This radiation is primarily nonthermal in origin.[7] The background brightness temperature in the vicinity of CP 1919 is about 55,000 degrees.

As explained in chapter 1, the spectral index for pulsars is not accurately known. However, from the data available it appears that the power spectrum of the sky background radiation has a steeper slope than the pulsar power spectrum. The slope of the background radiation is indicated in Figure 1-3 for comparison.

Therefore, at low frequencies the paramount problem is getting a high enough signal-to-noise ratio. A typical instantaneous bandwidth of pulsar signals is 10 kHz at 22 MHz (see Figure 3-1). Increasing the bandwidth of a receiver to more than the instantaneous bandwidth of the pulsar signal increases the noise level without increasing the signal level. On the other hand, the pulsar takes a longer time to sweep through a large bandwidth than through a small one, thereby increasing the available integration time per pulsar period. It is shown in Appendix A that the first effect is overwhelming, and that the optimum bandwidth for receiving pulsar signals is the instantaneous bandwidth of the pulsar. Now, in order to gain the maximum integration time per pulsar period, the centre frequency of the receiver can be swept so that it follows the frequency vs. time curve of the pulsar. The result is that the signal-to-noise power ratio is increased by a factor

$$\sqrt{\frac{\delta f}{B_i}}$$

over an optimum fixed bandwidth.

where δf is the sweep bandwidth of the receiver

B_i is the instantnaeous bandwidth of the pulsar

Because of the likelihood of gain fluctuations in the receiver a comparison source is used in the same way as in a Dicke receiver.[7] The comparison is the background noise. The receiver bandwidth follows the pulsar for one-half of the pulsar period, and repeats the sweep for the other half. Of course, the second time the receiver sees only background noise (see Figure 3-1). All the receiver parameters are the same for the first half as for the second half. The background noise is also the same for both sweeps. The receiver takes the difference between the outputs of two successive sweeps which is proportional to the pulsar signal strength.

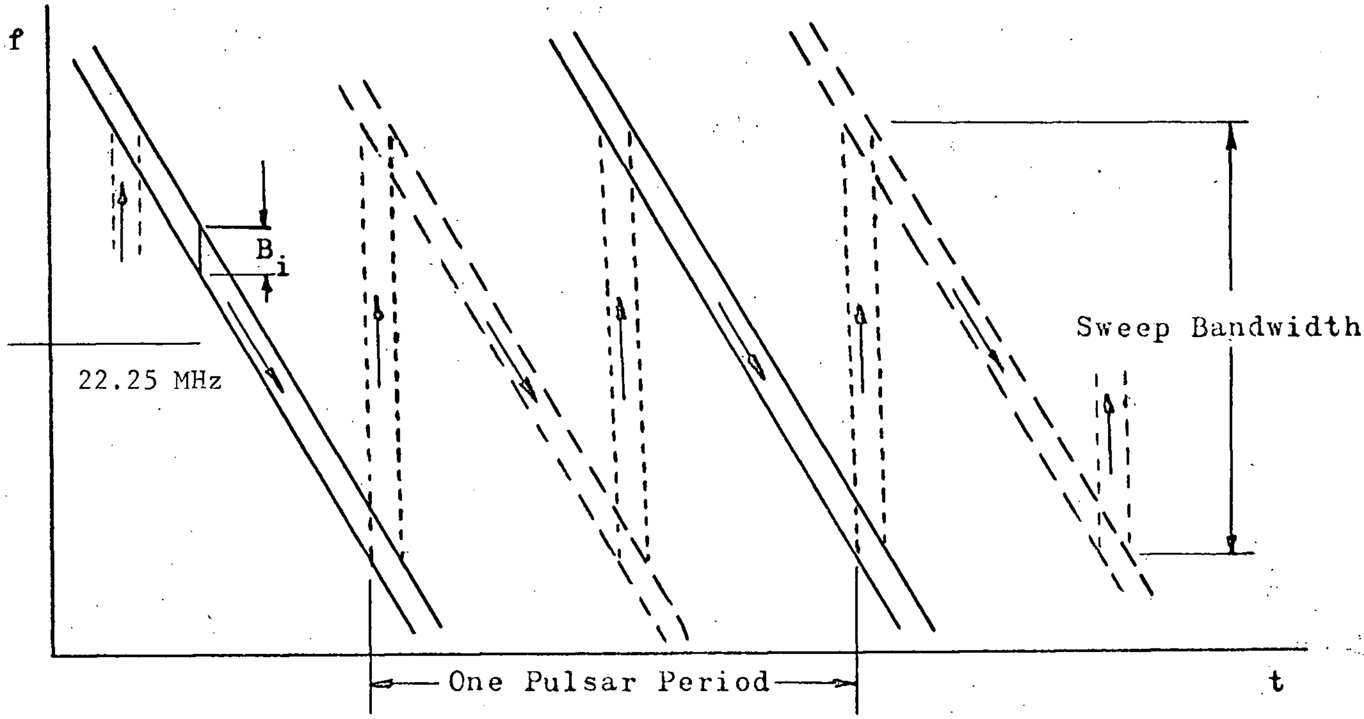

Figure 3-1
Arrows indicate the path followed by the receiver when it is in phase with the pulsar signal. For CP1919 the sweep bandwidth is 70.7 kHz and the instantaneous bandwidth (B_i) is 4.2 kHz. CP1919's heliocentric period is 1.3373011 seconds.

One important assumption that has been made is that the bandwidth sweep is in phase with the pulsar. If a search of the phases is required, then the gains in signal-to-noise ratio made by a sweeping bandwidth are nullified. However, any information about the phase can result in a higher probability of detection with a sweeping bandwidth. If observations are made simultaneously on a high frequency as well as at 22 MHz, the phase of the pulsar signal at 22 MHz can be predicted. Equation 1-1 can be integrated to give the time difference between the epoch at a high frequency and the epoch at 22 MHz. The time difference is directly proportional to the dispersion measure. This problem will be discussed again in chapter 6.

If the pulsars were a steadily pulsating phenomenon in which one pulse amplitude is statistically independent of the other amplitudes, the probability of detection could be increased by adding one pulse period to the next. However, it appears that they are not statistically independent, but occur in trains whose length is dependent upon the frequency.[9] For CP 1919 at 25 MHz strong pulse trains seem to last for about one minute on the average. Therefore, it is disadvantageous to integrate for times longer than the average time that a pulsar is active. At low frequencies the optimum integration time can only be guessed. The integration time used for CP 1919 was 30 seconds. Of course, longer integration can be obtained by a further averaging of the records.

It was decided to concentrate efforts on the pulsar CP 1919. At the time of year that observations were being made CP 1919 was transiting the meridian at night. At 22 MHz man-made interference restricts observations to between about 9:30 p.m. and 7:00 a.m. Also, CP 1919 has an accurately known dispersion measure. This accuracy is required in order to predict the phase of the pulsar signals at 22 MHz. CP 1919 has been seen at 40 MHz by Arecibo Ionospheric Observatory, and there has been considerable work done at higher frequencies.

4. THE ANTENNA

The antenna consists of the North-South arm of the 22 MHz T-shaped array used at D.R.A.O.[10] It is an array of 240 full-wave dipoles polarized in the East-West direction and mounted above a reflecting screen. The arm is 4λ wide, and its centre frequency is 22.25 MHz. It has a half-power beamwidth of 14 degrees in Right Ascension and 2.1 degrees in Declination at the zenith. Phasing of the individual rows of dipoles in the North-South arm by switching lengths of cable as delays provides steering in Declination, but not in Right Ascension.

Calibration of the sensitivity of the antenna was done by two methods. The first method was to point the antenna at the well-known, bright source Casseopeia A. Owing to the broadness of the beam (approximately one hour) in Right Ascension, several scans a few degrees in Declination on each side of Cass. A had to be made to provide a baseline. Cass. A is located in the plane of the Galaxy. The radiation from the Galaxy must be subtracted from the total in order to isolate the effect of Cass. A. Observations of Cass. A were further complicated by ionospheric scintillations which caused fluctuations of the order of a factor of two in the record. However, it has been shown that good flux densities can be determined even from scintillating records[11]. Comparison against a noise source substituted for the antenna was done in each case to get absolute values of noise temperature. This method gives the overall effective area including the ohmic loss factor for the feed cables in the antenna. Cass. A at 22 MHz has a flux density of 51,400 flux units (1 flux unit = 10^{-26} watts-m^{-2}-Hz^{-1}) and is randomly polarized.[12] The noise temperature due to this source at the input to the amplifier was compared with a standard and found to be 7000 degrees. The resulting sensitivity of the antenna is then 7.3 flux units per degree. The overall effective area is then

$$A_e = \frac{2kT}{S} = 376\ m^2.$$

There is a factor two because the antenna is receptive to only one polarization.

The aperture efficienay is then $\frac{\text{effective area}}{\text{physical area}} = 1.7\%$.

The other method is to look at the background sky. The region near the North Pole was chosen. This region has an average brightness temperature of 38,000 degrees at 22 MHz. The value of the brightness temperature at 22 MHz was obtained from the value at 38 MHz[8] using a spectral index of 2.50[6].

i.e.

$$\frac{T_{b1}}{T_{b2}} = \left(\frac{f_2}{f_1}\right)^{2.50}$$

where T_{b1} is the brightness temperature of the background at frequency f_1.

T_{b2} is the brightness temperature of the background at frequency f_2.

Because the output of the antenna is independent of the beam shape (as long as the beam is not so broad that the background sky can be considered to be an extended source of constant brightness temperature), this measurement gives the ohmic loss factor. The noise temperature at the input to the preamplifier was in this case measured to be 1180 degrees.

$$\text{Ohmic Loss Factor} = \frac{1180}{38,000} = 3.1\%$$

$$\text{Filling Factor} = \frac{\text{Overall Aperature Efficiency}}{\text{Ohmic Loss Factor}} = .548$$

The ohmic loss factor does not affect the signal-to-noise ratio significantly. Since most of the noise comes background sky, cable losses attenuate the signal and the noise equally. Very little extra noise is added by the cabling system in the antenna.

The filling factor, however, does affect this ratio because, in this case, only half of the geometrical area of the antenna can absorb signal power. But, as mentioned above, the output of noise power from the antenna is more or less independent of the shape of the antenna beam. The smaller antenna has the same noise power but less signal than the larger one.

5. THE SYSTEM

A block diagram of the system is shown in Figure 5-1. The 22 MHz antenna is connected to a preamplifier which is fed into an amplifier with a 3 db bandpass of 300 kHz centred at 22.250 MHz. It is mixed with a swept local oscillator centred at 32.950 MHz, and fed into an I.F. preamplifier and then a crystal filter. It is further amplified at 10.7 MHz and then detected. The detected output is amplified. The signal is then fed into a phase detector made from field-effect transistors, and then into an integrator which is discharged every 30 seconds. The output is displayed on a chart recorder. The timing is done by dividing down a 1 MHz crystal oscillator in the frequency synthesizer. The frequency of this was calibrated with the W.W.V.B. 60 kHz carrier. The timing control provides various triggering levels at the pulsar, as well as a 17-position, accurate digital delay. The delay can be used to trigger a frequency counter so that the output of the local oscillator can be checked at various points along the sweep.

Fortunately, the pulsar sweep is linear to a good approximation at 22 MHz. In a sweep corresponding to half a pulsar period CP 1919 deviates about 42 Hz from linearity at 22.25 MHz. This is only a small fraction of the 4.2 kHz instantaneous bandwidth of CP 1919. Therefore, a voltage ramp was used to control the output of the Hewlett-Packard frequency synthesizer as a local oscillator for the system. The non-linearity of the frequency synthesizer was more than that of the pulsar. It was measured to be a maximum of 400 Hz. This deviation is still only one tenth of the instaneous bandwidth of the pulsar.

In accordance with the method described in chapter 3, the reference (sky background) must be subtracted from the source plus reference (signal plus sky background). This subtraction is done by alternately switching the output into opposite inputs of a differential amplifier each pulsar half-period. Since all switching is done at twice the pulsar repetition rate, there is no possibility that a spurious timing signal can build up in the integrator. The off-periods of the phase detector are overlapped slightly so that during the period of possible transients,

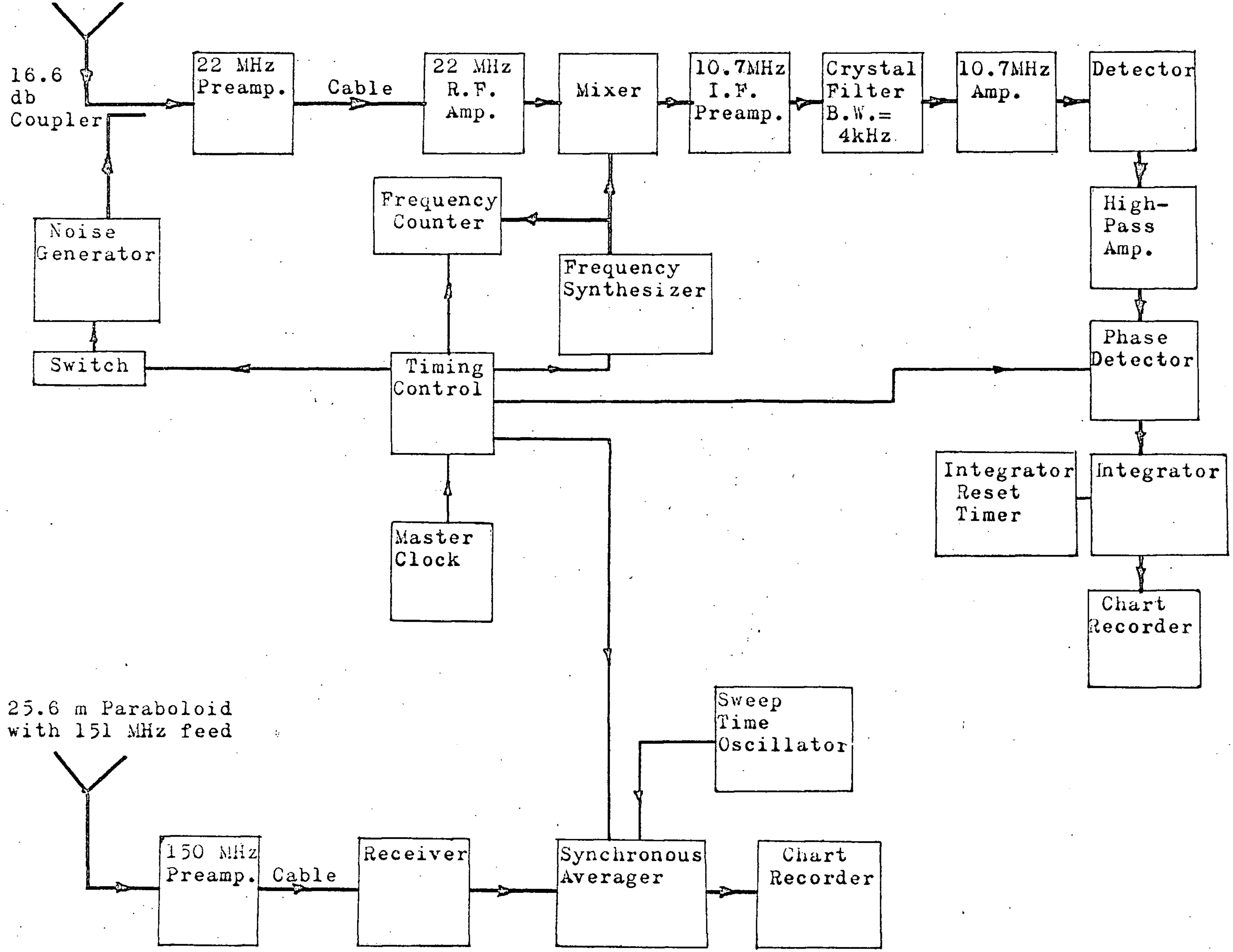
16.6 db Coupler
22 MHz Preamp.
Cable
22 MHz R.F. Amp.
Mixer
10.7MHz I.F. Preamp.
Crystal Filter B.W.= 4kHz
10.7MHz Amp.
Detector
Frequency Counter
Noise Generator
Frequency Synthesizer
High-Pass Amp.
Switch
Timing Control
Phase Detector
Integrator Reset Timer
Integrator
Master Clock
Chart Recorder
Sweep Time Oscillator
25.6 m Paraboloid with 151 MHz feed
150 MHz Preamp.
Cable
Receiver
Synchronous Averager
Chart Recorder

Figure 5-1

System Diagram: Thick lines represent R.F. paths and main signal paths. Thin lines represent paths of control signals.

Signals from Timing Control to:

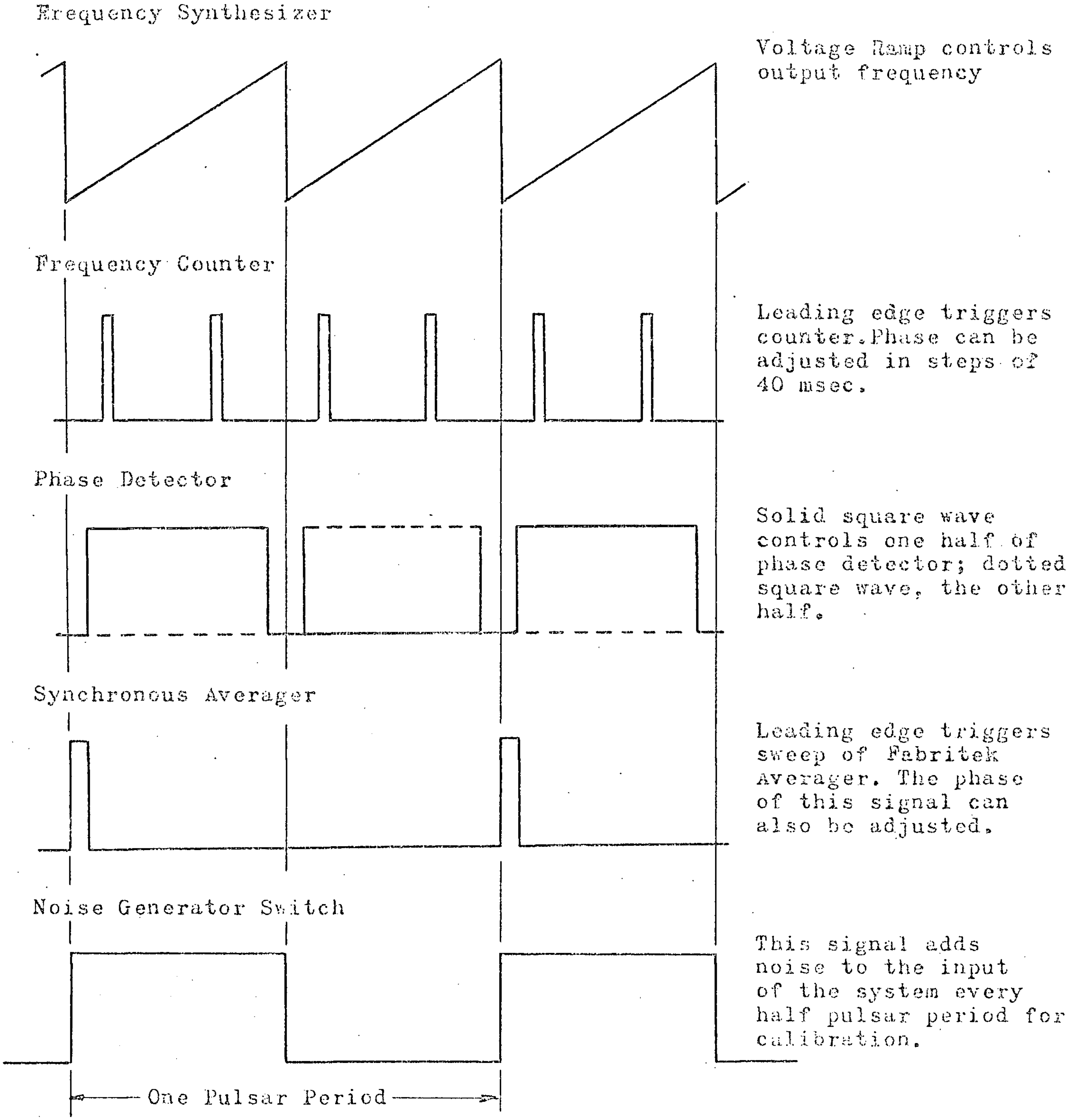

Figure 5-1

there is no signal coming out of the phase detector.

The sensitivity of the system can be calibrated by switching a noise on and off into the preamplifier synchronously with the sweep on alternate half-periods. The overall sensitivity will be discussed in chapter 7.

The 150 MHz antenna is the 26.5 m paraboliod located at D.R.A.O. A dipole feed is used with a Smythe preamplifier. The detected output is fed into a 256-channel signal averager arranged so that one sweep of the 256 channels is one pulsar period. A typical output from this system is shown in Figure 5-2. The sweep is triggered from the timing control in the 22 MHz system. The phase of the local oscillator sweep in the 22 MHz system can be adjusted relative to this trigger pulse.

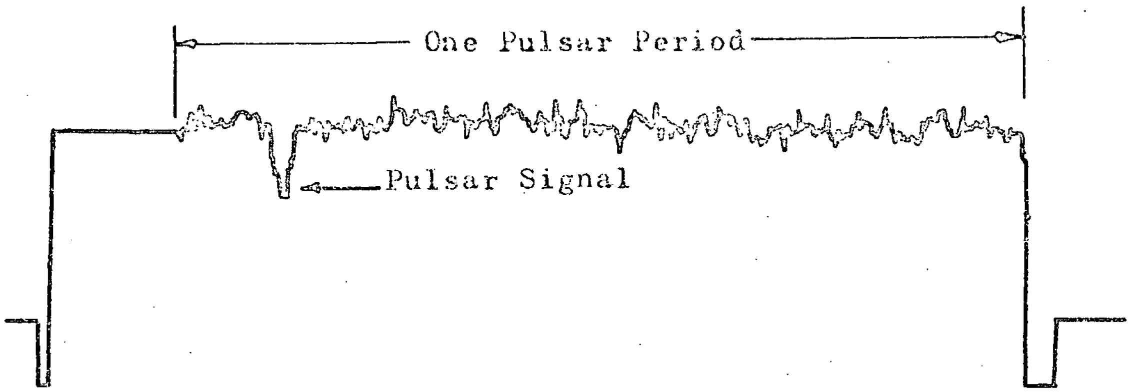

Figure 5-2
A typical 10 minute average from the 150 MHz system.

6. THE EXPERIMENT

As was pointed out in chapter 3, the bandwidth sweep must be in phase with the pulsar signal in order to get the full benefit of the system. It is possible to get the pulse epoch at a high frequency and use it to predict the phase at 22 MHz. The high frequency chosen was 151.5 MHz. The literature indicates(14) that the pulsar signals are likely to be strongest near 150 MHz. If observations are made simultaneously on the two frequencies then equation 1 can be integrated to give

$$t_{f2}-t_{f1} = 8.20\int n_e \, dL$$

where $f_2 = 151.5$ MHz

$f_1 = 22.250$ MHz.

For CP 1919 $t = 109.91$ seconds. The required phase change can easily be calculated.

Observations were made in this way on ten occasions. The phase of the local oscillator sweep was scanned during the observations to cover a range of about 100 msec on each of the predicted phase. This method was used as a compromise between searching all possible phases and spending the entire observing time at the predicted phase. Earlier observations were made during which all of the possible phases were scanned, but, as explained before, this method has no advantage over observing with a fixed bandwidth.

Figure 6-1 shows a typical piece of chart record made during the observations. The straight lines occur at the points when the integrator was reset (every 30 seconds). Therefore, the value of the output just before this point represents a 30 second average. The first section contains only background noise and the second section contains a simulated pulsar signal (see Figure 5-1) slightly larger than one standard deviation.

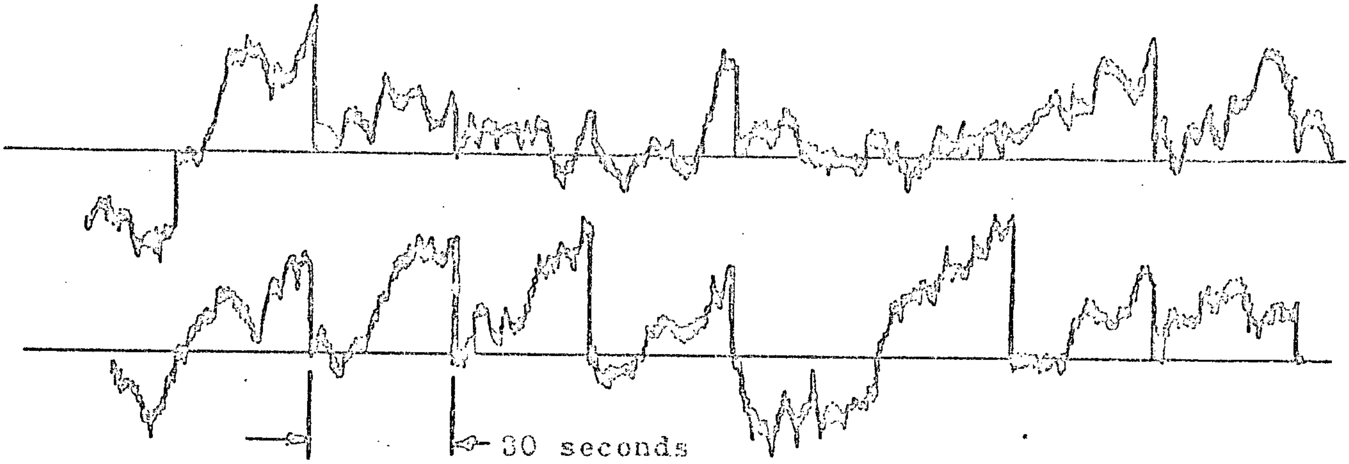

Figure 6-1

Output from the 22 MHz pulsar system. The upper trace is background noise; the lower one is background noise plus a simulated pulsar signal.

7. THE RESULTS

The minimum detectable brightness temperature will be determined by the background sky temperature and the receiver noise temperature. The noise temperature of the receiver was measured to be 200 degrees above ambient temperature. The background brightness temperature contributes 55,000 degrees ± 10,000 degrees in the region near CP 1919.[13] The efficiency with which this is transmitted to the preamplifier is 3.1%. Therefore,

$$T_s = \epsilon T_A + (1-\epsilon)T_o + T_R$$
$$= 2186 \text{ degrees}$$

where T_s is the overall system temperature

T_A is the antenna temperature

T_o is ambient temperature

T_R is the receiver temperature.

The standard deviation of the noise output is

$$\sigma = \frac{2\,T_s}{\sqrt{B\,\tau}}$$

where B is the I.F. bandwidth of the system

τ is the integration time.

For a single point on the record there is a 30 second integration time, and the bandwidth (chosen as the instantaneous bandwidth of CP 1919) is 4.0 kHz. Then,

$$\sigma = 12.6 \text{ degrees}.$$

This figure is somewhat lower than the measured standard deviation of 13.8 degrees (taken from 120 samples). The difference of approximately 10% is within the limits of accuracy of the calculations but could also be attributed to low-level, man-made interference. Since the sensitivity of the antenna is 6.9 flux units per degree and the pulse length of CP 1919 is 40 msec., then the standard deviation of the noise is 3.7×10^{-26} joules-m^{-2}-Hz^{-1} (expressed in the same units as pulsar intensity).

As explained in chapter 3 the integration can be done for longer periods than 30 seconds by averaging the records. The total time that the source is in the antenna beam is about one hour. If , as in a typical night's observations, 120 points are used, then

$$\sigma = 1.2 \text{ degrees.}$$

This standard deviation of noise corresponds toaa pulsar signal intensity of $.34\times10^{-26}$ joules-m^{-2}-Hz^{-1}.

APPENDIX

The optimum fixed bandwidth for receiving pulsar signals can be deduced as follows:

The receiver integrates pulsar signal power plus noise power over time T_1, and integrates the noise power over time T_0 (assuming that the receiver has a square law detector). The output voltage of the receiver, v, is the difference between these two integrations.

i.e. $\langle v\rangle = \langle v_1\rangle_{T_1} - \langle v_0\rangle_{T_0}$

If $\delta B < B$ $\quad v_1 = p\delta B + nB \quad$ (neglecting constants of proportionality)

$v_0 = nB$

where p is pulsar signal power per unit bandwidth

δB is the instantaneous bandwidth of the pulsar

B is the bandwidth of the receiver

The best signal-to-noise ratio is obtained when

$$\frac{\langle v\rangle^2}{\text{var } v}$$

is maximized. Since the two processes v_1 and v_0 are independent,

$$\text{var}\langle v\rangle = \text{var}\langle v_1\rangle_{T_1} + \text{var}\langle v_0\rangle_{T_0}$$

If v_1 and v_0 are assumed to be Gaussian, then

$$\text{var } v_0 = 2(nB)^2$$

$$\text{var } v_1 = 2(p\delta B + nB)^2$$

and $\quad \text{var}\langle v_0\rangle_{T_0} = \frac{\text{var } v_0}{2BT_0} = \frac{n^2 B}{T_0}$

If $p \ll n$ $\quad \text{var}\langle v_1\rangle_{T_1} = \frac{\text{var } v_1}{2BT_1} = \frac{n^2 B}{T_1}$

But $\quad T_1 = \frac{B}{df/dt} \quad$ and $T_0 = T - T_1$

where df/dt is the pulsar sweep rate

T is the pulsar period

Substituting $\quad \text{var}\langle v\rangle = n^2 \, df/dt \, (\frac{T}{T_0})$

Since $\langle v\rangle^2$ is $p^2 \delta B^2$ the bandwidth B should be as small as possible as long as $\delta B < B$.

If $\delta B > B$, then $\quad v_1 = (p + n) B$

and $\quad \frac{\langle v\rangle^2}{\text{var } v} = \frac{p^2}{n^2} \frac{T_1 \, df/dt}{1 + \frac{T_1}{T_0}}$

Therefore, T_1 or B should be made as large as possible as long as $B < \delta B$. Taking into account the above result, the optimum receiver bandwidth must be $B = \delta B$.

REFERENCES

1. Hewish, Bell, Pilkington, Scott, Collins, "Observations of a Rapidly Pulsating Radio Source", Nature, Vol. 217, Feb. 24, 1968, p. 709.
2. Davies, Smith, Hunt, "Changing Periodicities in the Pulsars", Nature, Vol. 221, Jan. 4, 1969, p. 27.
3. Drake, Gundermann, Jancey, Commella, Zeissig, Craft, "The Rapidly Varrying Radio Source in Vulpecula", Science, Vol. 160, May 3, 1968, p. 503.
4. Taylor, J.H., "Catalogue of 37 Pulsars", Astrophysical Letters, Vol. 3, 1969, p. 205.
5. Lovelace, Craft, "Intensity Variations of the Pulsar CP 1919", Nature, Vol. 220, Nov. 30, 1968, p. 875.
6. Bridle, A.H., "The Spectrum of the Radio Background Between 13 and 404 MHz", Monthly Notices of the R.A.S., Vol. 136, 1967, p. 219.
7. Kraus, John D., "Radio Astronomy", McGraw-Hill, 1966, p.236, p. 310.
8. Williams, Kenderdine, Baldwin, "A Survey of Radio Sources and Background Radiation at 38 MHz", Memoirs Royal Astronomical Society, Vol. 70, 1966, p. 53.
9. Robinson, Cooper, Gardiner, Wielebinski, Landecker, "Measurements of the Pulsed Radio Source CP 1919 between 85 and 2700 MHz", Nature, Vol. 218, June 22, 1968, p. 1143.
10. Costain, Lacey, Roger, "A Large 22 MHz Array for Radio Astronomy", I.E.E.E. Transactions on Antennas and Propagation, Vol. AP-17, No. 2, March, 1969, p. 162.
11. Purton, C.R., "The Spectra of Radio Sources and Background Radiation", Doctoral Thesis, University of Cambridge, June, 1966.
12. Roger, Costain, Lacey, "Spectral Flux Densities of Radio Sources at 22.25 MHz", Astrophysical Journal, Vol. 174, No. 3, April 1969, p. 366.

13. Galt, Costain, "Low-frequency Radio Astronomy", Transactions of the Royal Society of Canada, Fourth Series, Vol. 3, Sec. 3, 1965.

14. Wielebinski, R.,"Statistical Properties of Pulsar CP 1919", Nature, Vol. 219, Sept., 1968, p. 1135.

15. Lyne, Rickett, "Measurements of the Pülse Shape and Spectra of the Pulsating Radio Sources", Nature, Vol. 218, April, 1968, p. 329.